Robert Austin, Ephraim Buhks, Britton Chance, Don De Vault,
Paul Leslie Dutton, Hans Frauenfelder, and Vitalli I. Gol'danskii, Editors

Proceedings in Life Sciences

Protein Structure
Molecular and Electronic Reactivity

Springer-Verlag
New York Berlin Heidelberg
London Paris Tokyo

Electron Transfer Reactions in Bacterial Photosynthesis: Charge Recombination Kinetics as a Structure Probe

G. FEHER [a], M. OKAMURA [a], and D. KLEINFELD [b]

Introduction

During this conference the question of relevance to biology of the systems that were being investigated came up on several occasions. We are in the happy position of not having to defend our system on that score. Photosynthesis is essential to life; it is the source of energy of the entire living world.

Since this is the first talk on photosynthesis and reaction centers at this meeting, we shall start with a brief introduction to the subject. Photosynthesis deals with the conversion of light into chemical energy that is used by the organism to produce energy-rich compounds. The primary process of photosynthesis involves a charge separation, i.e., the formation of oxidized and reduced molecules. In photosynthetic bacteria this process occurs in a protein pigment complex called the reaction center (RC). The RC is composed of three polypeptide subunits called L, M, and H and a number of co-factors associated with the electron transfer chain. These are four bacteriochlorophylls (BChl), two bacteriopheophytines (i.e., a BChl without the central Mg), two ubiquinones (UQ-10) and one high-spin non-heme iron (Fe^{2+}) (for a review, see ref. 1).

Light induces a charge separation with an electron leaving the donor D, a specialized bacteriochlorophyll dimer, and passing via an intermediate acceptor, I, to the primary and secondary quinone acceptors, Q_A and Q_B, respectively (see Fig. 1); (for a review, see ref. 2). The remarkable thing about photosynthesis is that the quantum yield is close to unity. The high yield occurs because the forward reactions are 10^2–10^3 faster than the (energetically wasteful) charge recombinations reactions (see Fig. 1). We shall be hearing a great deal during this meeting about electron transfer reactions. We shall not discuss in detail the underlying theory here, but will mainly use one of the conclusions that seems to have been universally accepted by both theorists and experimentalists; namely, that *the kinetics of the electron transfer reactions are extremely sensitive to the spatial configuration of the charge separated species.* This enables us to use the kinetics as a

[a] Department of Physics B-019, University of California, San Diego, La Jolla, CA 92093.
[b] AT&T Bell Laboratories, Murray Hill, N.J. 07974.

structural probe. Although each of the transfer reactants can serve as such a probe we shall focus mainly on the recombination kinetics between D^+ and Q_A^- and D^+ and Q_B^-, characterized by τ_{AD} and τ_{BD}, respectively. We shall discuss the following topics:

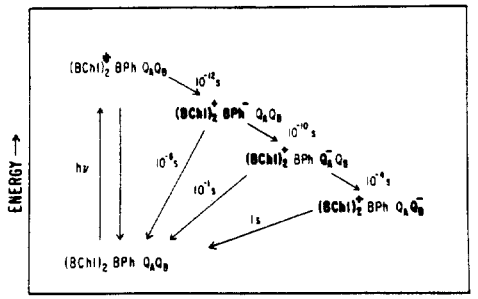

Figure 1 Schematic representation of the electron-transfer reactions in reaction centers from photosynthetic bacteria. After the absorption of a photon, the electron transfers through a series of reactants that are stabilized against charge recombination for progressively longer periods of time. Charged donor-acceptor species are in bold face. Transfer times are given for room temperature and are rounded to the nearest power of 10.

1. Do isolated RCs have the same structure as RCs *in vivo?*

2. The effect of removing the H-subunit on the charge recombination kinetics.

3. Conformational changes associated with the charge separation process.

4. The temperature dependence of the recombination kinetics.

5. The effect of electric fields on the recombination kinetics.

   a) Externally applied fields

   b) Fields due to intrinsic charges.

The first four topics deal with the relative spatial arrangement of the reactants; the fifth topic deals with the electronic level structure of the reactants.

1. Do isolated RCs have the same structure as RCs *in vivo* ?

Historically, the first complex that was called a reaction center was isolated by Reed and Clayton (3) and had a molecular weight of over one million. When we isolated a much smaller reaction center having a molecular weight of $\sim 10^5$, which resembled the "modern reaction center", we were astonished to find great opposition from several quarters when these findings were presented at the Gatlinburg Conference in 1970 (4). Some people just could not believe that such a small unit could perform the marvelous primary process of photosynthesis. They claimed that life had slipped through our fingers during the purification process and that these reaction centers probably bear little resemblance to what happens *in vivo*. Although this attitude has vanished by now, there still remain some lingering questions concerning the extent to which the isolated reaction centers have the same structures as RCs *in vivo*. We have, therefore, resurrected a table from an old piece of work by J. McElroy *et al.* (5) in which that question was addressed by measuring the charge recombination kinetics described by the scheme:

$$DQ_A \overset{h\nu}{\underset{\tau_{AD}}{\rightleftharpoons}} D^+Q_A^- \qquad (1)$$

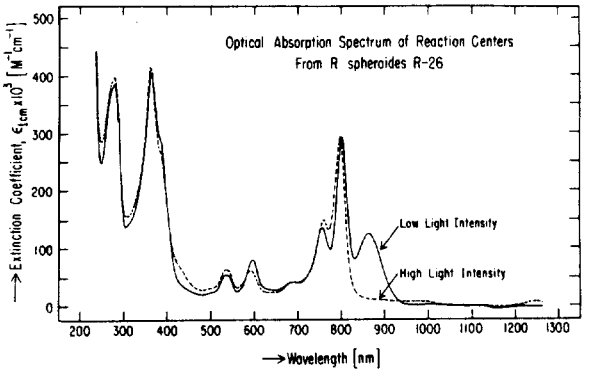

Figure 2 *Absorption spectrum of RCs from R. sphaeroides R-26 obtained under conditions of low light intensity (——) and with strong cross illumination (-----). The ordinate was normalized to the extinction coefficient at 802 nm, i.e.,* ($\epsilon^{802} = 2.88 \times 10^5 M^{-1}cm^{-1}$ *(6)). From Ref. 4.*

The state $D^+Q_A^-$ was formed by a short pulse of high intensity light. The charge recombination kinetics were monitored optically via changes in the absorption spectrum caused by the presence of D^+ (see Fig. 2). To prevent the electrons from leaving Q_A^-, these experiments were performed at 77 K. The results showed that whole cells, chromatophores and isolated reaction centers have, within experimental error, the same recombination time τ_{AD} * (see Table I). When reaction centers were

TABLE I. OPTICAL DECAY KINETIC OF WHOLE CELLS, CHROMATOPHORES, AND REACTION CENTERS OF *R. SPHAEROIDES*, R-26

Whole cells and chromatophores were suspended in 50% glycerol, 0.05 M Tris, pH 8.0, to give A_{800nm} *of approx. 0.1 (1 mm path). The presence of glycerol did not affect the kinetic behavior. It was used to insure the formation of a transparent glassy matrix of low temperatures. Reaction centers, unless otherwise specified, were suspended in the same buffer to give* A_{800nm} *of approx. 0.2 (1 mm path) at room temperature. Reaction centers which were exposed to 6 M urea for 4 h at 20°C in the dark had an absorbance* A_{800nm} *of approx. 1.0 (1 mm path). The decay of the optical change at 795 nm was monitored at a sample temperature of 80°K. The wavelength of the actinic illumination was 900 nm. The measuring beam intensity was approx. 5* $\mu W/cm^2$.

Preparation	1/e decay time	Treatment
Whole cells	30 ± 3 ms	No detergent
Chromatophores	32 ± 3 ms	No detergent
Reaction centers	29 ± 2ms	0.1% lauryl dimethylamineoxide
Reaction centers	52%, 28 ms, 48%, 93 ms	6 M urea, 0.1% lauryl dimethylamineoxide, $t = 4$ h
Reaction centers	60%, 260 ms, 40%, 1.8 s	0.1% sodium dodecylsulfate, 0.02% lauryl dimethylamineoxide

From: J. McElroy, D. Mauzerall, G. Feher (1974) Biochim. Biophys. Acta **333,** *261-277.*

treated with strong reagents (e.g., urea or sodium dodecyl sulfate) the decay kinetics changed significantly, indicating a structural change (see Table I). These experiments show that the structural integrity, at least with respect to the donor-acceptor complex, is preserved in isolated reaction centers.

2. The effect of removing the H-subunit

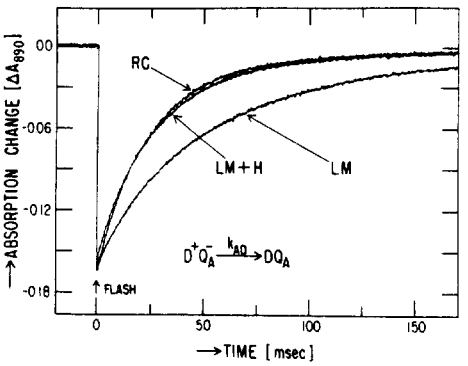

Figure 3 *Kinetics of charge recombination between Q_A^- and D^+ (k_{AD}) at cryogenic temperatures (77K). The formation and decay of the charge-separated state ($D^+Q_A^-$) was monitored at 890 nm following an actinic flash. From Ref. 7.*

All the prosthetic groups associated with the electron transfer processes are bound to the L and M subunits. The question concerning the role of the H subunit, therefore, naturally arises. R. Debus in our laboratory was able to isolate the LM-pigment-complex and the H-subunit and to subsequently reconstitute LM and H to reform RCs (7). When the charge recombination time, τ_{AD}, was measured at low temperatures, as discussed before, the results shown in Fig. 3 were obtained. The recombination times in LM were about a factor of two slower than those found in RCs. The recombination time between Q_A^- and D^+ is believed to be critically sensitive to changes in the distance between D and Q_A (5,8,9), a point that we shall discuss in more detail in the next section. Since τ_{AD} changes only by a factor of $\sim$ 2 (see Fig. 3), the relative configuration of D and Q_A is affected only to a relatively small extent by the removal of H. Thus, H does not play a major role in this charge recombination step. Incidently, note that the kinetics in the reconstituted LMH are practically identical to those in RCs. This shows that the change in the LM complex was not due to an irreversible denaturing effect accompanying the isolation procedure.

The charge recombination kinetics at room temperature in RCs containing *two quinones* exhibited a more dramatic change when H was removed. The kinetic properties of this system are described by:

$$DQ_AQ_B \underset{\tau_{AD}}{\overset{h\nu}{\rightleftharpoons}} D^+Q_A^-Q_B \underset{\tau_{BA}}{\overset{\tau_{AB}}{\rightleftharpoons}} D^+Q_AQ_B^- \qquad (2)$$

$$\tau_{BD}$$

In RCs or reconstituted LMH complexes the recombination time τ_{BD} was $\sim$ 1s, indicative

of the characteristic time of recombination between Q_B^- and D^+ (see Fig. 4). In LM, on the other hand, the recombination time was ten times shorter, as expected from the recombination between Q_A^- and D^+ (see Fig. 4). This suggests that the electron transfer from Q_A^- to Q_B was impaired. Indeed, independent experiments have shown that the electron transfer time, τ_{AB}, is about three orders of magnitude longer in LM than in RCs (7). This, of course, is a large effect that would likely be detrimental to the physiological well-being of the bacterium. From a structural point of view, this means that the distances (or angles) between Q_A and Q_B have been significantly changed upon removal of H. Another effect shown in Fig. 4 is the lack of recovery of the absorbance change in LM. This presumably is due to a loss of an electron to exogenous acceptors and may again be a consequence of the opening up of the structure.

3. Conformational changes associated with the charge separation process

There exists some evidence for bulk structural changes in the charge separated state. It comes from the calorimetric study of Arata and Parson (10,11) who found that during charge separation the volume of the RC-solvent system decreased. In a different set of experiments, Noks *et al.* (12) found that incubation of chromatophores with the cross-linker glutaraldehyde affected the electron transfer kinetics only if incubation was performed in the presence of light. We addressed the question of a conformational change during charge separation by analyzing the charge recombination kinetics in samples prepared under different conditions (13).

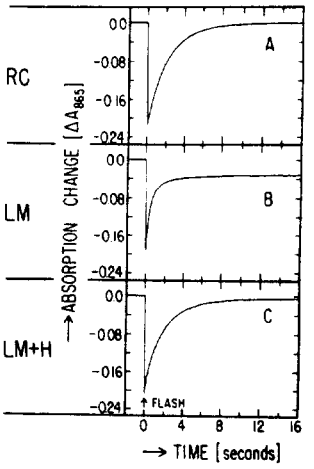

Figure 4 *Charge recombination between Q_A^- or Q_B^- and D^+ in RCs, LM, and reconstituted LMH at 4°C. The lack of complete recovery in the LM subunit is attributed to a loss of the electron from the quinone acceptors. From Ref. 7.*

We start by describing experiments performed on RCs containing only *one quinone*, i.e., we focus on the charge recombination between D^+ and Q_A^- (see Eq. 1). Two sets of samples were prepared. In one, RCs were cooled to cryogenic temperature under illumination, i.e., in the charge separated state. Thus any possible light-induced structural changes may be trapped when RC conformations are immobilized at low temperatures. The second sample was cooled to cryogenic temperature in the dark. The results of the kinetics of charge recombinations in the two samples is shown in Fig. 5a. There is a significant difference in the recombination time τ_{AD} between the two samples, i.e.,

$$\tau_{AD}^{light} = 120 \text{ ms}, \qquad \tau_{AD}^{dark} = 25 \text{ ms}.\ddagger$$

‡ The value of k_{AD} for UQ differs in recent RC preparations by $\sim$ 15% from that quoted earlier (see Table I) The origin of this discrepancy is not understood, it may be due to a changed binding site

In Fig. 5b the change of absorbence is plotted logarithmically; a single exponential recombination process should give a straight line on this plot. We see that RCs cooled under illumination have not only a longer recombination time, but their kinetics are much more non-exponential than those for RCs cooled in the dark. For comparison we show also the recombination kinetics at room temperature; in this case a good exponential recovery is observed.

Qualitatively, we attribute the non-exponential behavior to a distribution of structural states. Evidence that such distributions may exist in proteins comes from the detailed work of Austin, Frauenfelder and collaborators (14,15), and Woodbury and Parson (16). Furthermore, we see that RCs cooled under illumination deviate much more from exponentiality, i.e. they will have a broader distribution of conformational states. Their recombination time is also longer, indicating that the average distance between D^+ and Q_A^- has increased during illumination.

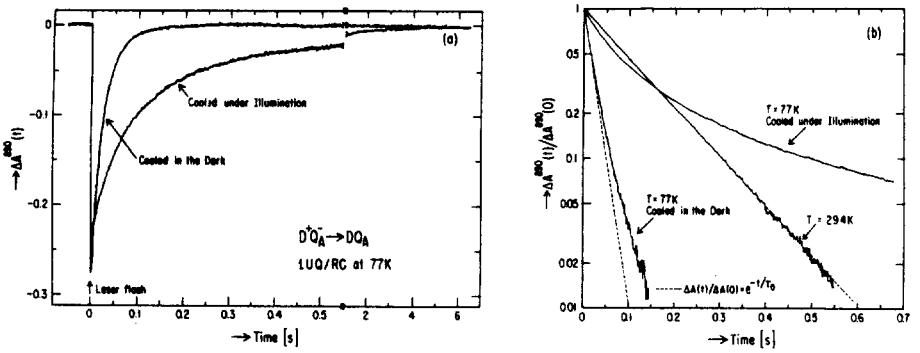

Figure 5 *Electron Donor Recovery Kinetics for 1UQ/RC following a laser flash. (a) Kinetics at 77K for RCs cooled in the dark and under illumination (b) semilog plot of the kinetics shown in part (a) together with kinetics obtained at room temperature. Dashed lines represent fits to an exponential function, with* τ_0 *= 22 ms for RCs cooled to 77 K in the dark and* τ_0 *= 132 ms for RCs at 294 K. Note the large deviation from an exponential of the kinetics in RCs cooled under illumination. From Ref. 13.*

To treat this problem quantitatively, we parameterize the recombination kinetics in terms of the D^+–Q_A^-electron transfer distance, r_{AD}. If all the donor acceptor pairs had identical separation distances, the observed absorption change would be given by a single exponential

$$\Delta A(t) \,/\, \Delta A(0) = e^{-t/\tau(r_{AD})} \tag{3}$$

where $\tau(r_{AD})$ is the characteristic recombination time, given by:

$$\tau(r_{AD}) = \tau_o e^{-r_{AD}/r_o} \tag{4}$$

the value of $r_o \simeq 1$Å (17,18). If r_{AD} varies between different donor acceptor pairs, Eq. 3 is no longer valid and $\Delta A(t)$ is described by a normalized distribution function of distances D(r), i.e.:

$$\Delta A(t) \,/\, \Delta A(0) = \int_0^\infty D(r) e^{-t/\tau(r)} dr \qquad (5)$$

To solve for the distribution function D(r), we fit the data with an analytic function given by:

$$\Delta A(t) \,/\, \Delta A(0) = [1 + t \,/\, (n\tau_o)]^{-n} \qquad (6)$$

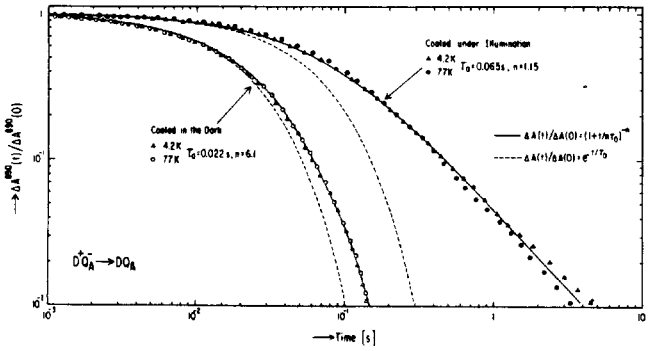

Figure 6 *Log-log plot of the donor recovery kinetics at 4.2 and 77 K in 1UQ/RC samples cooled in the dark and cooled under illumination. Dashed lines represent fits of the initial slopes of the data to an exponential; solid lines are fits to a power law (Eq. 6). The values of parameters* τ_o *and* n *are given in the figure. Note that* τ_o *is the same for both functions. From Ref. 18.*

This function is the same as used by Austin *et al* (14); it fits our data well as shown in Fig. 6. Equating this to the expression given by Eq. 5 one can solve for the distribution D(r), i.e.,

$$r_0 D(r) = \frac{1}{\Gamma(n)} \left[n \frac{\tau_0}{\tau(r)} \right]^n e^{-n[r_0/\tau(r)]} \qquad (7)$$

where $\Gamma(n)$ is the gamma function.

The result of the calculation of the distribution function is shown in Fig. 7. It bears out our qualitative discussion given before, i.e.:

1.) the average electron transfer distance in RCs cooled under illumination is larger than the average distance in RCs cooled in the dark,

2.) the width of the distribution in RCs cooled under illumination is two and a half times larger than in RCs cooled in the dark.

The shift and width of the distribution is of the order of 1Å, which is similar to the root mean square displacements determined from crystallographic studies on other proteins (19,20) and from model calculations (see, e.g., Refs. 21 and 22). The recombination kinetics were essentially temperature independent between 4.2 and 77 K (see Fig. 6). This indicates that the distribution remained constant with temperature, on the time scale, τ_{AD}, of the measurement.

It is interesting to speculate whether these light-induced changes have a physiological function analogous to those produced by allosteric changes in other proteins (for a review, see Ref. 23). Perhaps the structural changes accompanying the charge separation process

act to inhibit the wasteful recombination reactions by stabilizing the charge separated states. Such stabilization processes have also been discussed by Warshel (24), and Woodbury and Parson (16).

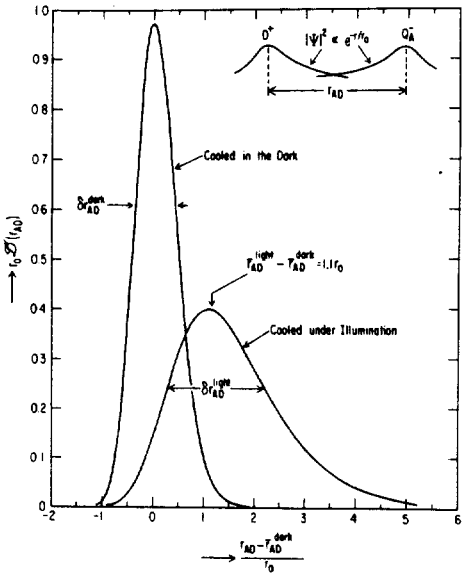

Figure 7 *Calculated distributions (see Eq. 7) of the electron transfer between* D^+ *and* Q_A^- *in 1UQ/RC samples cooled in the dark and under illumination. This distribution describes the nonexponential decay kinetics of* $D^+Q_A^-$*, shown in Figs. 5 and 6. The experimental parameters, n and* τ_0*, given in Fig. 6, were used together with Eqs. 4 and 7 to calculate the distributions. Insert shows the exponential decrease of the wave functions that leads to Eq. 4. Note that RCs cooled under illumination have a larger average electron-transfer distance as well as a larger spread in distances than RCs cooled in the dark. From Ref. 13.*

We now turn to the more complicated question of the recombination kinetics from the *secondary quinone*, Q_B, described by the scheme given by Eq. 2. The electron transfer time τ_{AB} is approximately 10^{-4}sec at room temperature but becomes unobservably long at 77 K. If we want to study, therefore, the recombination kinetics of $D^+Q_AQ_B^-$ at low temperature this state has to be trapped at 77 K by cooling RCs under illumination. This was done and the result of the recombination kinetics are shown Fig. 8. The solid line represents a theoretical fit to the same function as was used for the one quinone case (see Eq. 6). However, in this case one observes two features that are distinctly different from those observed in RCs containing one quinone. The recombination time is highly temperature dependent and the spread in characteristic times is very large. (Note the logarithmic scale of the abscissa). If we extrapolate the 18 K data to longer times the recombination is less than half complete even after 10^7s (1 year!).

The observed temperature dependence of the two quinone systems can be explained by the model of Agmon and Hopfield (25). Due to the dynamics of protein motion the RC passes through a number of structural states. The most favorable states for rapid recombination are those for which the distances between Q_B^- and D^+ are small. As the temperature is raised the probability that transitions to these favorable states occur is increased, thereby reducing the recombination time τ_{BD}. For RCs with one quinone the recombination time τ_{AD} is many orders of magnitude shorter than τ_{BD}. Consequently there is no opportunity to sample the different conformational states within the time τ_{AD}. This gives rise to an effective static distribution of distances between Q_A^- and D^+, resulting in temperature independent kinetics as observed in RCs with one quinone.

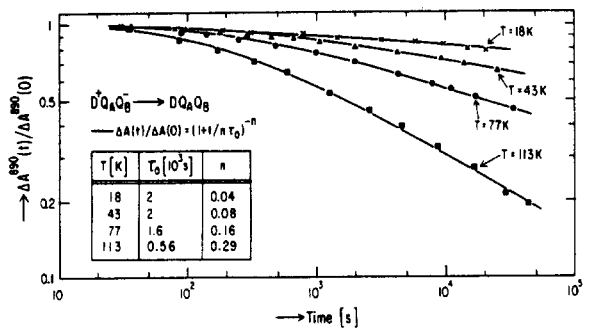

Figure 8 *Log-log plot of the donor recovery kinetics at different temperatures in 2UQ/RC samples cooled under illumination. Data were normalized to the maximum absorption change, $\Delta A^{890}(0)$, found by extrapolating the measured absorption changes back to zero time (more data were acquired at short times than are shown). The maximum absorption level [i.e., $A^{890}(\infty)$], which served as the base line for the absorption changes, was determined by warming and recooling the sample in the dark. Typically, $\Delta A^{890}(0)$ was 80% of $A^{890}(\infty)$. The parameters τ_0 and* n *were found from fitting the data to Eq. 6 and are tabulated in the insert. From Ref. 13.*

The above model also explains the exponential behavior found for τ_{AD} at room temperature. If the transitions between structural states occur in a time that is much shorter than τ_{AD}, the individual states will not be expressed and a single, average, τ_{AD} will be observed. This situation is analogous to motional narrowing in magnetic resonance.

An interesting finding that we will not discuss in detail here is that the electron transfer time from Q_A^- to Q_B is at least 8 orders of magnitude shorter in RCs that have been illuminated while being cooled as compared to those cooled in the dark (13). It is difficult to see how such a large change can be produced by a light-induced conformational change. It is more likely that a proton that associates with Q_B^- at room temperature (26) remains trapped in the vicinity of Q_B^- after the RCs are cooled. This proton cannot associate with RCs at low temperatures. Thus, RCs cooled in the dark will remain unprotonated upon illumination.

4. The temperature dependence of the recombination kinetics

We next discuss the temperature dependence of the charge recombination rate $D^+Q_A^- \rightarrow DQ_A$ (see Eq.1). We shall inquire whether the experimental results can be explained by present theories of electron transfer or whether major contributions are due to temperature dependent structural changes, e.g., thermal expansion.

Measurements were made using RCs containing one quinone, i.e., 1UQ/RC. All samples were cooled to cryogenic temperature in the dark; the value of k_{AD} was stable with time at each temperature and was completely reversible as the temperature was cycled.* To insure the presence of an optically transparent sample at all temperatures, RCs were incorporated into a thin film of polyvinyl alcohol (PVA) [27].

The temperature dependence of k_{AD} is shown in Fig. 9a. The recombination rate was essentially temperature independent at low temperature, as discussed earlier (see Fig.

*For RCs cooled under illumination, a different behavior of the kinetics was observed. Above ~ 90 K, k_{AD}^{light} changed with time heading, toward the value of k_{AD}^{dark}. Apparently, the structural changes that had been trapped during illumination were annealing out at T > 90 K.

6). As the temperature was increased from ~ 90 K to 300 K, k_{AD} decreased by a factor of ~ 6 † (see also Ref. 28-31). The results are similar to the temperature dependence of k_{AD} observed by Loach *et al.* [30] and Mar *et al.* [31] with RCs from *R. rubrum*. These temperature dependences are rather unusual; the rate k_{AD} *decreases* with *increasing* temperature. This is in contrast to the usual behaviour of thermally activated processes.

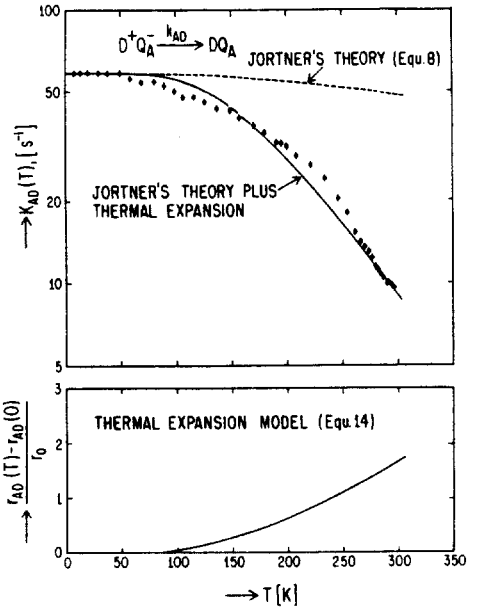

Figure 9 *a.) Temperature dependence of* k_{AD} *for 1UQ/RCs embedded in a 0.1mm polyvinyl alcohol film* (A^{800}=1.2). *Dashed line represents Jortner's theory (Eq. 8) with* $\Delta E_{redox}=E_{nuc}$ *and* T_o=500K. *Solid line represents the best fit of the expansion model (Eq.13,14) plus Jortner's theory to the experimental data. b.) Temperature dependence of the distance between* D^+ *and* Q_A^-, r_{AD}, *computed from the thermal expansion model (Eq.14).*

Can we understand the observed temperature dependence of k_{AD} in terms of the electron transfer theories of Hopfield [8] and Jortner [9,17]? In these theories, the electronic transition $D^+Q_A^- \rightarrow DQ_A$ is coupled to a vibrational mode(s) in the protein. The decrease in electronic energy during the charge recombination is compensated for by an equal increase in the energy of the vibrational mode coupled to the reaction. Thus, energy is conserved during the transition.

The theoretically predicted charge recombination rate can be expressed in a compact form under the approximation that both the electron donor and the acceptor are coupled to the *same*, single, vibrational mode. The recombination rate, valid for any temperature, T, is given by [9,17]:

$$k_{AD} = \frac{(2\pi)^2}{h}|M|^2 \frac{1}{k_B T_o}\left[\frac{\upsilon+1}{\upsilon}\right]^{p/2} e^{-s(2\upsilon+1)} I_p\left[2s\sqrt{\upsilon(\upsilon+1)}\right] \qquad (8a)$$

where

$$s = \frac{E_{nuc}}{k_B T_o} \qquad p = \frac{\Delta E_{redox}}{k_B T_o} \qquad \upsilon = \frac{1}{e^{T_o/T}-1} \qquad (8b)$$

The overlap integral M connects the electronic states of $D^+Q_A^-$ and DQ_A, T_o is the characteristic temperature of the vibrational mode (i.e., $k_B T_o = h\omega$), E_{nuc} is the energy required to rearrange the nuclear positions concomitant with the electron transfer, ΔE_{redox} is the

† The values for k_{AD} obtained with RCs in PVA are ~ 50% larger than those obtained with RCs in glycerol. This difference may be caused by the 1 Molar salt concentration in the dried PVA film.

difference in free energy between the D^+/D and Q_A/Q_A^- redox couples (i.e. the energy difference between $D^+Q_A^-$ and the ground state), $I_p(x)$ refers to the modified Bessel function of order p, k_B is Boltzman's constant and h is Plank's constant.

The temperature dependence of the predicted rate (Eqs. 8a and 8b) simplifies considerably in the limit of either high or low temperature. The recombinaton rate is expected to follow an activated temperature dependence when there is sufficient thermal energy available to excite the vibrational mode coupled to the reaction $D^+Q_A^- \rightarrow DQ_A$. In this limit, i.e., for $T >> T_o$, the rate is given by [8.9,17]:

$$\text{For } T>>T_o; \quad k_{AD} = \frac{(2\pi)^2}{h}|M|^2 \frac{1}{\sqrt{4\pi E_{nuc} k_B T}} e^{\frac{-(\Delta E_{redox}-E_{nuc})^2}{4E_{nuc}k_B T}} \tag{9}$$

At low temperature, i.e., for $T << T_o$, the vibrational mode coupled to the reaction remains in the ground state and thus the recombination rate is independent of temperature. In this limit, the rate is given by a Poisson distribution for the rearrangement energy, i.e. [9,17]:

$$\text{For } T<<T_o; \quad k_{AD} = \frac{(2\pi)^2}{h}|M|^2 \frac{1}{k_B T_o} s^p \frac{e^{-s}}{p!} \tag{10}$$

Note that for large p, the term p! in Eq.10 makes the low temperature limit of k_{AD} very sensitive to changes in the redox energy difference, E_{redox}, between $D^+Q_A^-$ and DQ_A. This limit applies to RCs, where $E_{redox} \sim 500$ meV [2] and $k_B T_o$ for proteins typically lies in the range 10 - 100 meV ($\sim$100 - 1000K).

The theoretical model we discussed predicts, in general, for temperatures near or above T_o an *increase* in the recombination rate with *increasing* temperature. This is in contradiction to the experimentally observed temperature dependence of k_{AD} (see Fig. 9a). A hypothesis often suggested (see, e.g., Refs.8,9,17) to circumvent this inconsistency between experiment and theory is that the redox energy difference between $D^+Q_A^-$ and DQ_A equals the nuclear rearrangement energy, i.e., $\Delta E_{redox} = E_{nuc}$. For this special condition, the theory predicts that k_{AD} is constant for $T<<T_o$ (see Eq. 10); and that k_{AD} *decreases* with *increasing* temperature for temperatures near of above T_o. For $T >> T_o$ and $p! >>1$, one obtains from Eqs.9 and 10 (with p! approximated by $\sqrt{2\pi p}\, p^p e^{-p}$) for the temperature dependence of k_{AD}:

$$\text{For } T>>T_o;\ p!>>1: \quad k_{AD} = k_{AD}(0)\sqrt{\frac{T_o}{2T}} \tag{11}$$

where $k_{AD}(0)$ is the low temperature limit of the recombination rate (see Eq. 10).

Since the observed recombination rate (see Fig. 9a) does not correspond to the high temperature limit we tried to fit the data with the general expression given by Eq. 8. We took the room temperature value of $\Delta E_{redox} = 500$ meV[2] and equated it to E_{nuc} (i.e., p

= s), with $k_{AD}(0) = 58\ s^{-1}$. To estimate T_o, we plotted k_{AD} *versus* T/T_o and found that T_o corresponds to $\sim$ 5 times the temperature at which k_{AD} changes from a temperature independent to a temperature dependent value. We see from Fig. 9a that this transition occurs at $\sim$ 100 K, i.e., the characteristic temperature is

$$T_o \sim 500\ K \tag{12}$$

Using the above values of T_o, ΔE_{redox}, E_{nuc} and $k_{AD}(0)$, the predicted temperature dependence of k_{AD} (Eq. 8) disagrees with the observed behaviour (Fig. 9a). Changing the value of E_{nuc} away from the value of E_{redox} increases the disagreement even further. For redox energies outside the range of 400 meV $> E_{nuc} >$ 700 meV (with E_{redox} = 500 meV), theory predicts a change in the *sign* of the temperature dependence, in accord with a thermally activated process. To reconcile the disagreement between experiment and theory, Sarai (32) and Kakitani *et al.* (33,34) modified the theories of Hopfield (8) and Jortner (9,17) by including a multiplicity of vibrational modes, as opposed to a single mode[†]. An alternate mechanism to account for the observed temperature dependence of k_{AD} is the thermal expansion of the protein (29,35,36). Thermal expansion will cause the donor-acceptor distance, r_{AD}, to increase with increasing temperature. This in turn will decrease the value of the overlap integral M, thereby reducing k_{AD} (see Eq. 4). To estimate the magnitude of this effect we write

$$|M(T)|^2 = |M(0)|^2\, e^{-|r_{AD}(T)-r_{AD}(0)|/r_o} \tag{13}$$

where r_o is the same scaling factor as used in Eq. 4. The change in lattice spacing for a simple solid with an anharmonic interatomic potential (see e.g. ref.37) is given by

$$\frac{r_{AD}(T)-r_{AD}(0)}{r_o} = \left[\frac{\gamma}{r_o}\right] \frac{T_o}{2} \left[\coth\frac{T_o}{2T} - 1\right] \tag{14}$$

where γ/r_o is an adjustable parameter related to the linear expansion coefficient, β, by $\beta=\gamma/r_{AD}(0)$. Assuming that the characteristic temperatures associated with the vibrational mode coupled to the thermal expansion is the same as that coupled to the electron transfer (i.e., T_o=500 K) we fitted the thermal expansion model (Eqs. 13, 14) to the observed data with a value of

$$\gamma/r_o = 1.4\times10^{-2}\ K^{-1} \tag{15}$$

This value corresponds to a thermal expansion coefficient that is an order of magnitude larger than that determined for a protein (38). It should be noted, however, that the relevant number is not the *average* expansion coefficient but the change in a *particular* distance, namely r_{AD} with temperature. This can be an order of magnitude larger that the change given by the average expansion coefficient (38).

[†] Now that the three dimensional structure of RCs is being determined (Deisenhofer *et al.* (1984) *J. Mol. Biol.* **180,** 385 and Michel *et al.*, these proceedings), there is hope that one will be able to correlate the vibrational mode(s) with specific bonds in the vicinity of the primary reactants.

The temperature dependence of r_{AD} found from the expansion model is shown in Fig. 9b. The change in r_{AD} between low temperature and room temperature is $\Delta r_{AD}=1.7r_o\sim 1-2$ Å. This is the same as found for some atomic positions in a protein (38). Thus, the expansion mechanism seems to provide a possible mechanism for the temperature dependence of k_{AD}, although it certainly does not constitute a proof.

Before leaving this topic let us briefly discuss the assumption that $\Delta E_{redox} = E_{nuc}$. At first glance it seems odd that nature should have picked this equality since it maximizes the rate (k_{AD}) of a physiologically undesirable reaction. However, this constraint may be a consequence of maximizing the transfer rate for the forward reaction $D^+I^-Q_A \rightarrow D^+IQ_A^-$, where I is the intermediate acceptor (2). The redox energy difference between the I/I^- and Q_A/Q_A^- redox couples is approximately the same as that between the Q_A/Q_A^- and D^+/D couples (2).

The temperature dependence of k_{AD} in *R. rubrum* (30,31) was found to be similar to that observed in *R. sphaeroides* (Fig. 9a). However, Mar *et al.* (31) found a much weaker temperature dependence of k_{AD} in RCs from *Ectothiorhodospira* sp. The simplest explanation of this result is that in this bacterial species $\Delta E_{redox} \neq E_{nuc}$, although the alternate explanation that the temperature dependence of Δr_{AD} has been reduced cannot be excluded.

Can we test experimentally the applicability of the electron transfer theories to RCs, and in particular, whether our assumption $\Delta E_{redox} = E_{nuc}$ is justified? Eq. 8 predicts a parabolic-like dependence of k_{AD} verus ΔE_{redox} with k_{AD} peaking at $\Delta E_{redox} = E_{nuc}$. Thus the most direct test would be to vary ΔE_{redox} and to establish whether k_{AD} exhibits the expected parabolic dependence. ΔE_{redox} was changed by substituting quinones with different redox potentials for the native ubiquinone (39).

The low temperature (77K) values of k_{AD} are plotted together with the theortical curve (Eq.10) in Fig.10 with the assumption that $\Delta E_{redox}(UQ)=E_{nuc}$. The redox potentials of the quinones were taken from ref. (40); the accepted value ΔE_{redox} for UQ is 520 meV (11). The general parabolic feature of the theory are seen to be borne out by the experimental data. However, it should be kept in mind that the redox potentials used were obtained for quinones in dimethylformamide at *room* temperature and are likely to deviate from the values found in situ (41) at low temperatures. Furthermore, substitution of quinones may change other parameters (e.g. r_{AD}) besides ΔE_{redox} that affect k_{AD}. Consequently a quantitative agreement of the experimental results with theory cannot be expected at this point; the rather good agreement shown in Fig. 10 seems to us better than one has the right to expect.

An extensive and systematic set of substitution experiments have been performed by

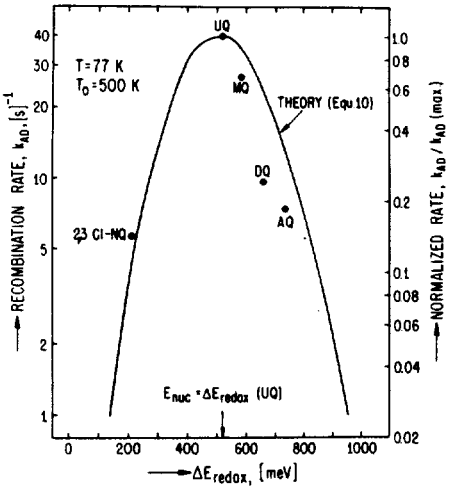

Figure 10 *The low temperature recombination rate, k_{AD}, as a function of ΔE_{redox}. Solid line represents Jortner's theory (Eq.10) with T_o=500K and $E_{nuc}=\Delta E_{redox}$ = 520 meV. Dots represent experimental points obtained with RCs in which the native ubiquinone (UQ) was substituted with different quinones. The values of k_{AD} for menadione (MQ), duroquinone (DQ) and anthraquinone (AQ) were taken form ref. (39), the value for 2,3, dichloronaphtoquinone (2, 3Cl-NaQ) represents a new measurement. The values of the redox potentials were taken from ref. (40).*

Gunner *et al.* (42). They reported that at room temperature the value of k_{AD} was essentially constant over a large range ($\sim$ 0.7 eV) of redox potentials. These results seemed to be in disagreement with electron transfer theories as was pointed out during this conference. However, more recently, these authors concluded (43) that their room temperature measurements on the halogenated benzoquinones did not represent a direct recombination process but a transfer of electrons via excess quinones in solutions. Measurements of k_{AD} at low temperatures would eliminate this problem and would provide additional important data to compare with theory. An alternate way of changing ΔE_{redox} is to apply an external electric field across the reaction center as discussed next.

5. The effect of electric fields on the recombination kinetics

Before discussing the effect of an electric field on the direct recombination rate, k_{AD}, we shall consider the case in which the electric field changes the observed recombination via an indirect pathway. Thus, we shall discuss now how the kinetics can be used to probe *electronic energy levels* rather than *conformational changes*.

Fig. 11 shows the electron transfer reactions that we will be concerned with (44) The state $D^+IQ_A^-$ can decay via a direct or indirect pathway, as indicated. The observed decay rate of this state, k_{obs}, is in general a combination of the direct and indirect pathways. Assuming that the rates k_{AI} and k_{IA} are fast in comparison to k_{ID} and k_{AD}, the states $D^+I^-Q_A$ and $D^+IQ_A^-$ can be considered to be in equilibrium and the observed decay rate is given by:

$$k_{obs} = k_{INDIRECT} + k_{DIRECT} = k_{ID}\alpha + k_{AD}(1-\alpha) \qquad (16)$$

where α is the fraction of RCs in the thermally excited state $D^+I^-Q_A$ (see Fig.10). For $\alpha << 1$, the condition that prevails in RCs, Eq. 16 becomes

$$k_{obs} \simeq \alpha k_{ID} + k_{AD} = k_{ID}e^{-\Delta G^o/k_bT} + k_{AD} \qquad (17)$$

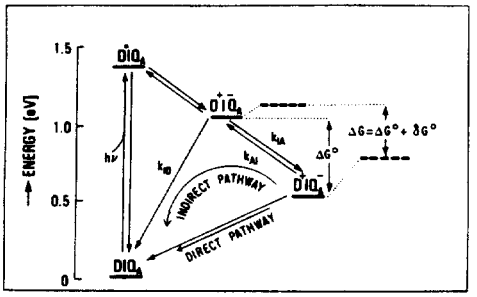

Figure 11 *Simplified energy level scheme showing electron transfer (arrows) in reaction centers of R. sphaeroides. The state $D^+IQ_A^-$ can decay either via the direct pathway (with rate k_{AD}) or via the intermediate state $D^+I^-Q_A$, depending on the value of the energy difference, ΔG° (Eq. 17). An electric field changes ΔG° by δG° and affects, therefore, the recombination rate via the indirect pathway (Eq. 18). The change in energy levels, is illustrated for a direction of the electric field that reduces ΔG°. When the field is reversed, the energies of the two states are lowered and ΔG° is increased. From Ref. 44.*

Which of the two pathways predominates depends critically on the value of the energy difference ΔG°. Substituting the measured values of k_{ID} and k_{AD} into Eq. 17 one can show that the two pathways will contribute equally, i.e., $k_{DIRECT} = k_{INDIRECT}$, for $\Delta G^\circ = 400$ meV. The energy gap, ΔG°, in RCs containing the native ubiquinone (UQ) as the primary acceptor has been determined to be 500 - 600 meV (40,45) while for anthraquinone (AQ) $\Delta G^\circ = 340$ meV (40,44,46). Since one of these numbers is larger and the other smaller than the critical value of 400 meV, the direct pathway predominates for UQ whereas the indirect pathway predominates for AQ.

a.) Externally applied fields.

Effect on the indirect pathway: We shall first focus on RCs that have anthraquinone as the primary acceptor; in this case the observed (indirect) recombination rate will be given by the first term of Eq. 17, i.e.:

$$k_{obs} = k_{ID}e^{-\Delta G^\circ/k_bT} \tag{18}$$

Let us now consider the effect of an electric field on the energy levels. The two states $D^+I^-Q_A$ and $D^+IQ_A^-$ will be effected to a different extent since the magnitudes of their dipoles along the electric field are different. This is indicated by the dashed lines in Fig. 11. The energy difference between the two states has been changed by an amount δG° producing a change in the recombination rate given by

$$k_{obs} = k^\circ_{obs}e^{-\delta G^\circ/k_bT} \tag{19}$$

where k°_{obs} is the recombination rate in the absence of an electric field.

How is an electric field applied across the RCs? A. Gopher in our laboratory incorporated RCs into a lipid bilayer that separates two aqueous compartments (44,47). A voltage was applied across the bilayer and the current produced by the charge recombination following a pulse of light was measured. Fig. 12 shows the results of such an experiment performed on RCs containing AQ. The top panels show the current measured after the light is turned off, i.e. during the charge recombination process. The areas under the

curves represent the total transferred charge and are, therefore, equal in all three panels. Consequently, the amplitude increases as the recombination time becomes shorter. In the lower panel the experimental data are plotted logarithmically. The data were fitted with a straight line given by

$$\tau = 1/k_{obs} = 8.5\times10^{-3}e^{-V/0.175}\ s \qquad (20)$$

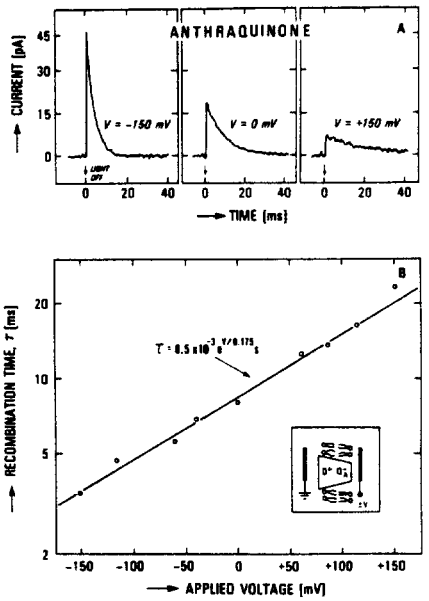

Figure 12 *The effect of an applied electric field on the kinetics of charge recombination in RCs with anthraquinone as the primary acceptor incorporated in a planar bilayer. A.) Time course of current after light pulse is turned off in the absence (V=0) and presence (V=±155mV) of an electric potential. B.) Dependence of the charge recombination rate on the applied voltage. Solid line represents least square fit to the data and obeys the relation* $\tau = 8.5\times10^{-3}e^{V/0.175}$s. *Inset shows the polarity of the voltage with respect to the functionally oriented population of RCs. The polarity of the output signal was inverted by an amplifier. From Ref. 44.*

We see that an e-fold change in the recombination time, τ, results when the applied voltage across the membrane is 175 mV. If I and Q_A were to span the entire membrane one would expect an e-fold change for 25 mV (i.e., k_bT/q), where q is the charge of the electron. The fact that we need a seven times larger voltage means that the component of the distance between I and Q_A along the normal of the membrane is only 1/7th of the width of the membrane.

It is interesting to speculate whether the effect of an electric field on the recombination kinetics has any physiological significance. We know that the outside of chromatophores is negative with respect to the inside and that the RCs are oriented in the membrane with the donors pointing towards the inside. Thus the membrane potential created during charge separation *in vivo* decreases ΔG°, thereby decreasing the quantum efficiency at high light intensity. Thus, nature may have build in a negative feedback to prevent detrimental effects at high light intensities.

Effect on the direct pathway: Let us now consider the case of RCs containing UQ. Since now ΔG° is larger than the critical value of 400 meV, the direct pathway predominates. Fig. 13 shows that the recombination kinetics remained uneffected within experimental error (±5%) over the range of applied voltages (±150meV). How do we reconcile this result with electron transfer theories? If we assume again that $\Delta E_{redox} = E_{nuc}$, then k_{AD} is relatively insensitive to changes in ΔE_{redox} (i.e., $[dk_{AD}/d(\Delta E_{redox}-E_{nuc})]=0$). Under these conditions, Eq.8 predicts that for a 10% change in k_{AD} one needs a change in

($\Delta E_{redox} - E_{nuc}$) of $\sim$ 200 meV (see Fig.10). Although we have applied 300 meV across the membrane, the effective voltage across the $D^+Q_A^-$ dipole is reduced by the ratio of the projection of the distance between D^+ and Q_A^- along the field to the thickness of the membrane. This will reduce the effective voltage below the required 200 meV. Thus, the experimental results are compatible with theory if $\Delta E_{redox} - E_{nuc}$ is close to zero.

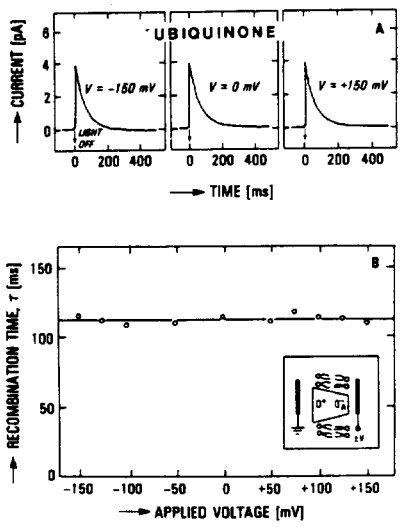

Figure 13 *The effect of an applied electric field on the kinetics of charge recombination in RCs with ubiquinone (UQ-10) as the primary acceptor. Compare the results with those shown in Fig. 12. (Note the difference in time scales and the logarithmic ordinate). From Ref. 44.*

We plan to repeat these experiments and determine k_{AD} with higher precision (48). We will also attempt to apply higher (pulsed) voltages to the membrane. If $\Delta E_{redox} - E_{nuc}=0$, the change in k_{AD} should be approximately independent of the direction of the electric field (note the near symetry of the theoretical curve in Fig.10). If $\Delta E_{redox} - E_{nuc} \neq 0$, k_{AD} should pass through a maximum for one field direction when the voltage across $D^+Q_A^-$ equals $(\Delta E_{redox} - E_{nuc})/q$.

Z. Popovic *et al.* reported at this conference experiments in which they applied considerably larger fields to RCs embedded in monolayers deposited on a substrate (see also ref. 49). Changes in k_{AD} have been observed although the analysis of the data is complicated by the fact that the RCs are randomly oriented and the decay has to be deconvoluted into a number of exponentials.

b) Fields due to intrinsic charges.

Instead of applying an electric field from an external source, we can also explore the effect of electric fields produced by charges associated with the protein. In particular, we can investigate the protonation of the quinones, a problem that has so far not been solved satisfactorily (see, e.g., Refs. 50-52).

The rationale of the experiment is as follows: The proton produces an electric field, thereby shifting the energy levels of $D^+I^-Q_A$ and $D^+IQ_A^-$ as described previously (see Fig. 11). This produces a change in k_{obs} given by the relation (in analogy to Eq. 19):

$$k_{obs}^{H^+} = k_{obs}^{\circ}\, e^{-\delta G^{\circ}/k_b T} \qquad (21)$$

where $k_{obs}^{H^+}$ and k_{obs}° are the recombination rates in the presence and absence of a proton and δG° is the energy shift caused by the binding of the proton.

As the pH is varied, k_{obs} should change in accordance with the pK value for the pro-

$$k_{obs} = \frac{k^{o}_{obs} + 10^{(pK-pH)} k^{H^+}_{obs}}{1 + 10^{(pK-pH)}} \qquad (22)$$

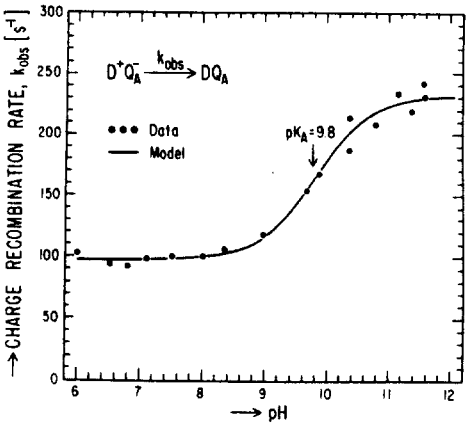

Figure 14 *The pH dependence of the charge recombination rate* k_{obs}. *The solid line (Model) was calculated using Eq. 22 with* pK_A = 9.8, $k^{H^+}_{obs}$=97s^{-1} *and* k^{o}_{obs}=230s^{-1}. *From Ref. 59.*

Fig. 14 shows the pH dependence of k_{obs} in RCs containing AQ (53). The solid line represents a theoretical fit (Eq. 22) with k^{o}_{obs}=230 s^{-1}, k^{H+}_{obs}=97 s^{-1} and pK = 9.8. The value of pK is in agreement with that found from redox titrations (54-56) and electron transfer measurements (26).

The interaction energy δG^{o} obtained from Eq. 21 is 22 meV. From this value one can make a rough estimate of the location of the proton binding site relative to Q_A^-. Assuming that the interaction of the proton with both Q_A^- and I^- is electrostatic in origin, one calculates a distance that is *larger* than $\sim$ 5 Å. Additional experiments are in progress to obtain this distance from ENDOR experiments on Q_A^- in RCs (57,58).

Summary:

We have shown how electron transfer reactions can be used to probe the spatial and electronic structure of photosynthetic reaction centers. Both "static" strcutural changes (e.g., produced by removal of the H subunit) and "dynamic" changes (e.g., produced by illumination) as well as the effect of an electric field on the energy levels were investigated. Several findings (e.g., the temperature dependence of the recombination kientics and the lack of dependence of an electric field on the recombination kinetics) can be reconciled with present theories of electron transfer reactions by assuming that the difference in redox energy, ΔE_{redox} is approximately equal to the reorganization energy, E_{nuc}. Additional experiments were suggested to investigate the validity of this assumption. The temperature dependence of the recombination kinetics was explained by a thermal expansion model. Although we have focused in this work only on a particular charge recombination reaction, the approach should be applicable to other electron transfer reaction as well.

Acknowledgement:

We gratefully acknowledge the contributions of the many students, post-docs and collaborators whose work was cited in this review. The work from our laboratory was supported by grants from the NIH (GM-13191) and NSF (DMB 82-02811).

NOTE ADDED IN PROOF

On the Determination of the Characteristic Temperature, T_o.

Bixon and Jortner (59) have tried to fit the temperature dependence of k_{AD} (see Fig. 9) with a characteristic frequency $h\omega = 100\ cm^{-1}$ (i.e. $T_o \simeq 140K$), which is considerably lower than the one we used (Eq. 12). Although their fit at temperatures below 200K is good, they fail to fit the temperature dependence between 200 and 300K. There is, of course, no justification (except simplicity) to fit the entire temperature dependence with one value of T_o, since the vibrations involved in the electron transfer are likely to be different from those associated with the expansion. In the absence of information about the characteristic temperatures of either set of vibrations, we had opted in Fig. 9 for the simple approach of fitting the entire temperature range with a single temperature, T_o. We have now been able to determine the characteristic temperature of one of the vibrations that we believe plays a role in the electron transfer and thus fit the observed temperature dependence of k_{AD} in a more logical way.

The vibrations in question are those of the hydrogens bonded to the two oxygens of the primary acceptor, Q_A (57,58) (see insert in Fig. 15). We have determined the temperature dependence of the O--H bond length by measuring the hyperfine interaction of the proton with the unpaired spin on Q_A^- (60). This interaction has been shown to be dipolar (58,61), i.e., it is proportional to r^{-3}, where r is the O-H bond length. Thus, for small changes, Δr, in the bond length, the change in the hyperfine coupling, ΔA, is given by

$$\frac{\Delta A}{A} \simeq -3\,\frac{\Delta r}{r} = -3\left(\frac{\Delta r}{r_o}\right)\left(\frac{r_o}{r}\right) \quad (23)$$

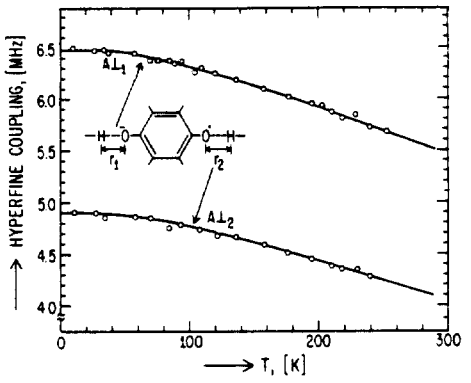

Figure 15 Temperature dependence of the perpendicular components of the hyperfine couplings ($A_\perp$) of the exchangeable protons on Q_A^- (57,58). Solid line represents the theoretical fit (Eq. 24) with $T_o = = 200K$ and $\gamma/r_o = 4.0 \times 10^{-4}\ K^{-1}$ and $4.8 \times 10^{-4}\ K^{-1}$ for $A_{\perp 1}$ and $A_{\perp 2}$, respectively.

Substituting Eq. 14 for $\Delta r/r_o$ yields

$$\frac{\Delta A_{1,2}}{A_{1,2}} = -\frac{3}{2}\,\frac{\gamma_{1,2}}{r_{1,2}}\,T_o\left[\coth\frac{T_o}{2T} - 1\right] \quad (24)$$

where the subscripts 1 and 2 refer to the two protons. The temperature dependence of the perpendicular component of the hyperfine interaction, $A_\perp$, of both protons is shown in Fig. 15. The solid line represents a fit of the data to Eq. 24 with $T_o = 200K$, $\gamma_1/r_o = 4.0 \times 10^{-4}\ K^{-1}$, $r_1 = 1.55Å$, $\gamma_2/r_o = 4.8 \times 10^{-4}\ K^{-1}$, $r_2 = 1.71Å$. Thus, the characteristic temperature is closer to the value favored by Bixon and Jortner (59). From

the sensitivity of the fit to T_o we estimate a possible error in T_o of $\pm$ 50K.

We next have to show that the O-H vibration is involved in the electron transfer reaction under discussion (Eq. 1, Fig. 9). The evidence comes from the isotope effect, i.e., the observed change in k_{AD} when the protons were substituted with deuterons (62). The experimentally determined value of k_{AD} increased at 300K by 6% upon deuteration. A simple theoretical argument showed that in the low temperature limit a 20% effect is expected (62). At $T = 300K$ and $T_o = 200K$ Eq. 8 predicts an order of magnitude smaller isotope effect. Notwithstanding the lack of quantitative agreement between the observed and predicted isotope effect, we take the qualitative agreement as evidence that the hydrogen bonding protons associated with Q_A provide a vibrational mode that is important in the electron transfer reaction.

Having determined the characteristic temperature, T_o^{ET}, of the vibrations coupled to the electron transfer, we leave the other characteristic temperature, T_o^{exp}, associated with the expansion as well as the expansion coefficient γ/r_o as free parameters to fit the observed temperature dependence of k_{AD} with the expression (obtained from Eq. 8 and 14)

$$k_{AD}(T) = k_{AD}(0)\tanh^{\frac{1}{2}}\left(\frac{T_o^{ET}}{2T}\right) e^{-\frac{\gamma T_o^{exp}}{2r_o}\left(\coth\frac{T_o^{exp}}{2T} - 1\right)} \qquad (25)$$

where $\tanh^{\frac{1}{2}}\left(\frac{T_o^{ET}}{2T}\right)$ is the strong coupling limit ($s \gg 1$) of Eq. 8a. It is plotted in Fig. 16 (dashed line) for $T_o^{ET} = 200K$. A fit of Eq. 25 to the experimental data (dots) with $T_o^{ET} = 200K$, $T_o^{exp} = 1000K$ and $\gamma/r_o = 0.036$ is shown by the solid line in Fig. 16. Although the fit is very good, the high value of γ/r_o is cause for concern. The expansion mechanism invoked probably represents an oversimplification of the situation; other mechanisms may contribute to the temperature dependence of k_{AD}. Clayton for instance, showed that k_{AD} in dehydrated RCs at $T = 300K$ has a value that is similar to the one observed at cryogenic temperatures (63). Similarly, we have found that k_{AD} of RCs in PVA films that have been thoroughly dehydrated by prolonged pumping fitted the dashed line of Fig. 16 (Eq. 8) rather than the solid line (Eq. 25) (64). Thus, the water of hydration must play an important role in the electron transfer. Clayton suggested that the

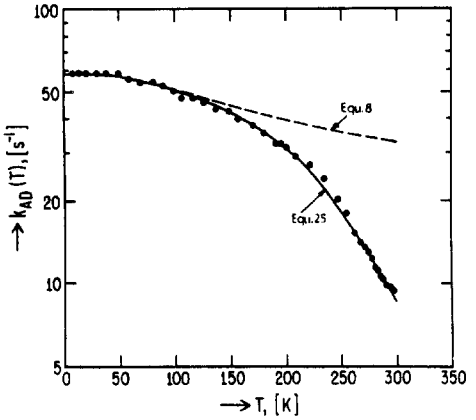

Figure 16 Temperature dependence of k_{AD}. Experimental data (dots) same as in Fig. 9. Solid line represents the best fit of eq. 25 with $T_o^{ET} = 200K$, $T_o^{exp} = 1000$, $\gamma/r_o = 0.036$. Dashed line represents Yortner's theory (eq. 8) with $\Delta E_{redox} = E_{max}$ and $T_o^{ET} = 200K$.

observed temperature dependence is due to a phase transition of the bound water (63). The orientational polarizability of the water dipoles may represent another mechanism. It should also be noted that the distance between Q_A^- and D^+ is rather large ($\sim$ 20Å) and consequently encompasses a large amount of protein structure. Any temperature dependent characteristic of the intervening space (e.g. a change in the conformation of the protein backbone) may contribute to the observed temperature dependence. X-ray structure analyses of RCs from *R. sphaeroides* performed at different temperatures should shed some light on this question (65,66).

References

1. Feher, G. and Okamura, M. Y.; in *The Photosynthetic Bacteria,* R. K. Clayton and W. R. Sistrom, eds. (Plenum Press, N.Y.), chapter 19, pp. 349-388 (1978).
2. Parson, W. W. amd Ke, B. (1982) In *Photosynthesis: Energy Conversion by Plants and Bacteria* (Govindjee, ed.), pp. 331-385, Academic Press, New York.
3. Reed D. W., and Clayton, R. K. (1968), *Biochim. Biophys. Res. Commun.* **30,** 471-475.
4. Feher, G. (1971) *Photochem. & Photobiol.* **14,** #3 (Supplement #1), 373-388.
5. McElroy, J. D., Mauzerall, D. C., and Feher, G. (1974) *Biochim. Biophys. Acta,* **333,** 261-277.
6. Straley, S. C., Parson, W. W., Mauzerall, D. C., and Clayton, R. K. (1973) *Biochim. Biophys. Acta* **305,** 597-609.
7. Debus, R. J., Feher, G. and Okamura, M. Y. (1985) *Biochemistry* **24,** 2488-2500.
8. Hopfield, J. J. (1974) *Proc. Natl. Acad. Sci. USA* **71,** 3640-3644.
9. Jortner, J. (1976) *J. Chem. Phys.* **64,** 4860-4867.
10. Arata, H. and Parson, W. W. (1981) *Biochim. Biophys. Acta* **636,** 70-81.
11. Arata, H. and Parson, W. W. (1981) *Biochim. Biophys. Acta* **638,** 201-209.
12. Noks, P. P., Lukashev, E. P., Kononenko, A. A., Venediktov, P. S., and Rubin, A. B. (1977) *Mol. Biol. (Moscow)* **11,** 1090-1099.
13. Kleinfeld, D., Okamura, M. Y., and Feher, G. (1984) *Biochemistry* **23(24),** 5780-5786.
14. Austin, R. H., Beeson, K. W., Eisenstein, L., Frauenfelder, H., and Gunsalus, I. C. (1975) *Biochemistry* **14,** 5355-5373.
15. Frauenfelder, H. (1978) *Methods Enzymol.* **54,** 506-532.
16. Woodbury, N. W. T. and Parson, W. W. (1984) *Biochim. Biophys. Acta* (in press).
17. Jortner, J. (1980) *J. Am. Chem. Soc.* **102,** 6676-6686.
18. Redi, M., and Hopfield, J. J. (1980) *J. Chem. Phys.* **72,** 6651-6660.
19. Frauenfelder, H., Petsko, G. A., and Tsernoglou, D. (1979) *Nature (London)* **280,** 558-563.
20. Artymiuk, P. J., Blake, C. C. F., Grace, D. E. P., Patley, S. J., Phillips, D. C., and Sternberg, M. J. E. (1979) *Nature (London)* **280,** 563-568.
21. Karplus, M, and McCammon, J. A. (1981) *CRC Crit. Rev. Biochem.* **9,** 293-349.
22. Levitt, M., Sander, C., and Stern, P. S. (1985) *J. Mol. Biol.* **181**, 123-447.
23. Huber, R., and Bennett, W. S. (1983) *Biopolymers* **183,** 261-679.
24. Warshel, A. (1980) *Proc. Natl. Acad. Sci. USA* **77,** 3105-3109.
25. Agmon, N. and Hopfield, J. J. (1983) *J. Chem. Phys.* **78,** 6947-6959; **80,** 592 (erratum).
26. Kleinfeld, D., Okamura, M. Y., and Feher, G. (1984) *Biochim. Biophys. Acta* **766,** 126-140.

27. Eisenberger, P., Okamura, M. Y., and Feher, G. (1983) *Biophys. J.* **37,** 523-538.
28. Parson, W. W. (1967) *Biochim. Biophys. Acta* **153,** 248-259.
29. Hsi, E. S. P. and Bolton, J. R. (1974) *Biochim. Biophys. Acta* **347,** 126-133.
30. Loach, R. A., Kung, M., and Hales, B. J. (1975) *Ann. NY Acad. Sci,* **244,** 297-319.
31. Mar, T., Vadeboncoeur, C., and Gingras, G. (1983) *Biochim. Biophys. Acta* **724,** 317-322.
32. Sarai, A. (1980) *Biochim. Biophys. Acta* **589,** 71-83.
33. Kakitani, T. and Kakitani, H. (1981) *Biochim. Biophys. Acta* **635,** 498-514.
34. Kakitani, T. and Mataga, N. (1985) *J. Phys. Chem.* **89,** 8-10.
35. Hales, B. J. (1976) *Biophys. J.* **16,** 471-480.
36. Hopfield, J. J. (1976) *Biophys. J.* **16,** 1239-1240.
37. Feynman, R. P. (1972) *Statistical Mechanics: A set of Lectures,* pp. 53-55, W. A. Benjamin, Reading, PA.
38. Ringe, D., Kuriyan, J., Petsko, G. A., Karplus, M., Frauenfelder, H., Tilton, R. F., and Kuntz, I. D. (1984) *Am. Crystallographic Assoc. Transactions* **20,** 109-122.
39. Okamura, M. Y., Isaacson, R. A., and Feher, G. (1975) *Proc. Natl. Acad. Sci.* **72** #9, 3491-3495.
40. Prince, R. C., Gunner, M. R., Dutton, P. L. in *Function of Quinones in Energy Conserving Systems,* B. L. Trumpower, ed., Academic Press, Inc., New York., pp. 29-33 (1982).
41. Recently, N. W. Woodbury, W. W. Parson, M. R. Gunner, R. C. Prince, and P. L. Dutton (1986) *Biochim. Biophys. Acta* **851,** 6-22, have determined the redox potentials of different quinones *in situ* from the quantum yield of delayed fluorescence. They found significant deviations from the values determined in dimethylformamide. Unfortunately, their data were also obtained at room temperature and are, therefore, not strictly applicable to the data of Fig.10. We are indebted to N. W. Woodbury and W. W. Parson for making their data available to us prior to publication.
42. Gunner, M. R., Tiede, D. M., Prince, R. C., and Dutton, P. L. in *Function of Quinones in Energy Conserving Systems,* B. L. Trumpower, ed., Academic Press, Inc., New York., pp. 265-269 (1982).
43. Gunner, M. R. (private communication).
44. Gopher, A., Blatt, Y., Schönfeld, M., Okamura, M. Y., and Feher, G. (1985) *Biophys. J.* **48,** 311-320.
45. Arata, H., and Parson, W. W. (1981) *Biochim. Biophys. Acta* **638,** 201-209.
46. Gunner, M. R. Y., Liang, Y., Nagus, D. K., Hochstrasser, R. M., and Dutton, P. L. (1982) *Biophys. J. (Abstracts)* **37,** 226a.
47. Schönfeld, M., Montal, M., and Feher, G. (1979) *Proc. Natl. Acad. Sci. USA* **76,** 6351-6355.
48. We have recently been able to measure changes in k_{AD} with a precision of $\sim 0.5\%$ [M. Y. Okamura and G. Feher (1986) *Biophys. J. (Abstracts)* **49**, 587a].
49. Popovic, Z. D., Kovacs, G. J., Vincett, P. S., and Dutton, P. L. (1985) *Chem. Phys. Letters* **116,** 405-410.
50. Crofts, A. R. and Wraight, C. A. (1983) *Biochim. Biophys. Acta* **726,** 149-185.
51. Maroti, P. and Wraight, C. (1985) *Biophys. J. (Abstracts)* **47,** 5a.
52. Kleinfeld, D., Okamura, M. Y., and Feher, G. (1985) *Biochim. Biophys. Acta* **809,** 291-310.
53. Kleinfeld, D., Okamura, M. Y., and Feher, G. (1985) *Biophys. J.* **48,** 849-852.
54. Prince, R. C. and Dutton, P. L. (1976) *Arch. Biochem. Biophys.* **172,** 329-334.
55. Rutherford, A. W. and Evans, M. C. W. (1980) *FEBS Lett.* **110,** 257-261.
56. Wraight, C. A. (1981) *Isr. J. Chem.* **21,** 348-354.
57. Lubitz, W., Abresch, E. C., Debus, R. J., Isaacson, R. A., Okamura, M. Y., and Feher, G. (1985) *Biochim. Biophys. Acta* **808,** 464-469.

58. Feher, G., Isaacson, R. A., Okamura, M. Y., and Lubitz, W. (1985) *Antennas and Reaction Centers of Photosynthetic Bacteria: Structure, Interaction and Dynamics* (M. Michel-Beyerle, ed.) Springer-Verlag, Berlin, pp. 174-189.

59. Bixon, M., and Jortner, J. (1986) *J. Phys. Chem.* **90**, 3795-3800.

60. Feher, G., Isaacson, R. A., Okamura, M. Y. and Lubitz, W. (1986), unpublished results.

61. O'Malley, P. J., Chandreshekar, T. K. and Babcock, G. T., *Antennas and Reaction Centers of Photosynthetic Bacteria: Structure, Interaction and Dynamics* (M. Michel-Beyerle, ed.) Springer Verlag, pp. 339-344.

62. Okamura, M. Y. and Feher, G., *Proc. Natl. Acad. Sci. USA* (1986) **83**, 8152-8157.

63. R. K. Clayton (1978). *Biochim. Biophys. Acta* 504, 255-264.

64. Arno, T. R., McPherson, P. H., Feher, G. (1986), unpublished results.

65. Allen, J. P., Feher, G., Yeates, T. O. and Rees, D. C. (1986) presented at the VIIth International Congress on Photosynthesis, Brown University, *Proceedings*, Martinus Nijhoff/W. Junk (in press).

66. Allen, J. P., Feher, G., Yeates, T. O., Rees, D. C., Deisenhofer, J., Michel, H and Huber, R. *Proc. Natl. Acad. Sci.* (1986) **83**, 8589-8593.

Acknowledgements

Table 1 and Figure 2 (on page 401) are reprinted from Feher, G. (1971) *Photochem. & Photobiol.* 14(3, Suppl. 1), 373–388, with the permission of Elsevier/North Holland Biomedical Press, Amsterdam, and with the permission of Pergammon Press, Elmsford, New York, respectively.

Figures 5, 6, 7, and 8 (on pages 404, 405, and 407, respectively) are printed from Kleinfield, D., Okamura, M.Y., and Feher, G. (1984) *Biochemistry* 23(24), 5780–5786, with the permission of the American Chemical Society, Washington, D.C.

Figures 11, 12, and 13 (on pages 413, 414, and 415, respectively) are reprinted from Gopher, A., Blatt Y., Schönfeld, M., Okamura, M.Y., and Feher, G. (1985) *Biophys. J.* 48, 311–320, with the permission of The Rockefeller University Press, New York, New York

Figure 14 (on page 416) is reprinted from Kleinfeld, D., Okamura, M.Y., and Feher, G. (1985) *Biophys. J.* 48, 849–852, with the permission of The Rockefeller University Press, New York, New York.